THE JOURNAL OF BIOLOGICAL CHEMISTRY VOL. 283, NO. 42, pp. 28020–28028, October 17, 2008

Proteinase-activated Receptor 2 Stimulates Na,K-ATPase and Sodium Reabsorption in Native Kidney Epithelium*

Received for publication, June 9, 2008, and in revised form, July 25, 2008 Published, JBC Papers in Press, August 4, 2008, DOI 10.1074/jbc.M804399200

Luciana Morla[‡§], Gilles Crambert[‡§], David Mordasini[‡§], Guillaume Favre[‡§1], Alain Doucet[‡§2,3], and Martine Imbert-Teboul[‡§2]

From the [‡]Université Pierre et Marie Curie, Univ Paris 06, UMR 7134, 75005 Paris and the [§]CNRS, UMR 7134, the Laboratoire de Physiologie et Génomique Rénales, Institut des Cordeliers, 75006 Paris, France

Proteinase-activated receptors 2 (PAR2) are expressed in kidney, but their function is mostly unknown. Since PAR2 control ion transport in several epithelia, we searched for an effect on sodium transport in the cortical thick ascending limb of Henle's loop, a nephron segment that avidly reabsorbs NaCl, and for its signaling. Activation of PAR2, by either trypsin or a specific agonist peptide, increased the maximal activity of Na,K-ATPase, its apparent affinity for sodium, the sodium permeability of the paracellular pathway, and the lumen-positive transepithelial voltage, featuring increased NaCl reabsorption. PAR2 activation induced calcium signaling and phosphorylation of $ERK_{1,2}$. PAR2-induced stimulation of Na,K-ATPase V_{max} was fully prevented by inhibition of phospholipase C, of changes in intracellular concentration of calcium, of classical protein kinases C, and of $ERK_{1,2}$ phosphorylation. PAR2-induced increase in paracellular sodium permeability was mediated by the same signaling cascade. In contrast, increase in the apparent affinity of Na,K-ATPase for sodium, although dependent on phospholipase C, was independent of calcium signaling, was insensitive to inhibitors of classical protein kinases C and of $ERK_{1,2}$ phosphorylation, but was fully prevented by the nonspecific protein kinase inhibitor staurosporine, as was the increase in transepithelial voltage. In conclusion, PAR2 increases sodium reabsorption in rat thick ascending limb of Henle's loop along both the transcellular and the paracellular pathway. PAR2 effects are mediated in part by a phospholipase C/protein kinase C/$ERK_{1,2}$ cascade, which increases Na,K-ATPase maximal activity and the paracellular sodium permeability, and by a different phospholipase C-dependent, staurosporine-sensitive cascade that controls the sodium affinity of Na,K-ATPase.

Proteinase-activated receptors (PARs)[4] constitute a unique class of the seven-transmembrane domain G protein-coupled receptors. Their ligand, tethered in their extracellular domain, is unmasked upon cleavage of their N-terminal domain by specific proteases (1). To date, four isoforms of PARs (PAR1–4) displaying different profiles of activation by serine proteases have been cloned. PAR1, PAR3, and PAR4 are activated by thrombin, whereas PAR2 is activated by trypsin. PARs can also be activated experimentally, without proteolysis, by synthetic peptides that mimic their ligand domain.

PAR1 and PAR2 are expressed in most tissues, where their stimulation is coupled to the activation of phospholipase C (PLC) β and, secondarily, to that of various protein kinases C (PKCs), which often trigger $ERK_{1,2}$ phosphorylation (2–4). Besides PLCβ, PAR1 and PAR2 may also activate other signaling pathways in a tissue-specific manner (4).

Although PAR1 and PAR2 are expressed at high level in the kidney (5–8), their effects on renal function remain mostly unknown. PAR1 has been involved in inflammatory cell-mediated renal injury in crescentic glomerulonephritis (9, 10), and PAR2 has been involved in the development of interstitial fibrosis in IgA nephropathy (7). PAR1 and PAR2 have also been shown to induce vasoconstriction and vasodilatation of renal vessels, respectively, thereby decreasing and increasing glomerular filtration rate (11). However, whether they exert a physiological effect on epithelial cells function has not been established. PAR2 may be involved in the control of kidney ion transport because 1) it is expressed in renal tubule epithelial cells (5), 2) in many epithelia, including distal colon, pancreatic duct, and airways, activation of PAR2 induces chloride secretion through activation of calcium-dependent channels (12–16), and 3) similar observations have been made in M1 cells, a mouse cell line derived from renal collecting duct principal cells (5). It must be stressed, however, that the renal epithelium is a reabsorptive and not a secretory epithelium and that native renal tubule epithelia display neither chloride secretion nor apical calcium-sensitive chloride channels.

Thus, we investigated the role of PAR2 in the regulation of solute transport in a native kidney epithelium and its signaling pathway. In preliminary experiments in rat kidney, we found a high level of PAR2 mRNA expression along the whole renal tubule. This study was focused on the rat cortical thick ascending limb of Henle's loop (cTAL), a nephron segment that avidly

* This work was supported by a grant from Amgen (2005/29-N). The costs of publication of this article were defrayed in part by the payment of page charges. This article must therefore be hereby marked "*advertisement*" in accordance with 18 U.S.C. Section 1734 solely to indicate this fact.

[1] Present address: INSERM U145, Nice, France.

[2] Both authors contributed equally to this work.

[3] To whom correspondence should be addressed: 15 rue de l'Ecole de Médecine, 75270 Paris cedex 6, France. Fax: 33-1-46-33-41-72; E-mail: alain.doucet@bhdc.jussieu.fr.

[4] The abbreviations used are: PAR, proteinase-activated receptors; ERK, extracellular signal-regulated kinase; MAP, mitogen-activated protein; PLC, phospholipase C; PKA, cAMP-dependent protein kinase; PKC, protein kinase C; cPKC, classical PKC; CaMK, calmodulin kinase; MLC-K, myosin light chain kinase; PD_{te}, transepithelial potential difference; AP, agonist peptide SLIGRL-NH_2; F-AP, furoylated derivative of AP; RP, reverse inactive peptide LRGILS-NH_2; TAL, thick ascending limb of Henle's loop; cTAL, cortical TAL; BAPTA, 1,2-bis(o-aminophenoxy)ethane-*N*,*N*,*N*′,*N*′-tetraacetic acid; AVP, vasopressin; ROMK, rectifying, voltage-insensitive potassium channels; Try, trypsin.

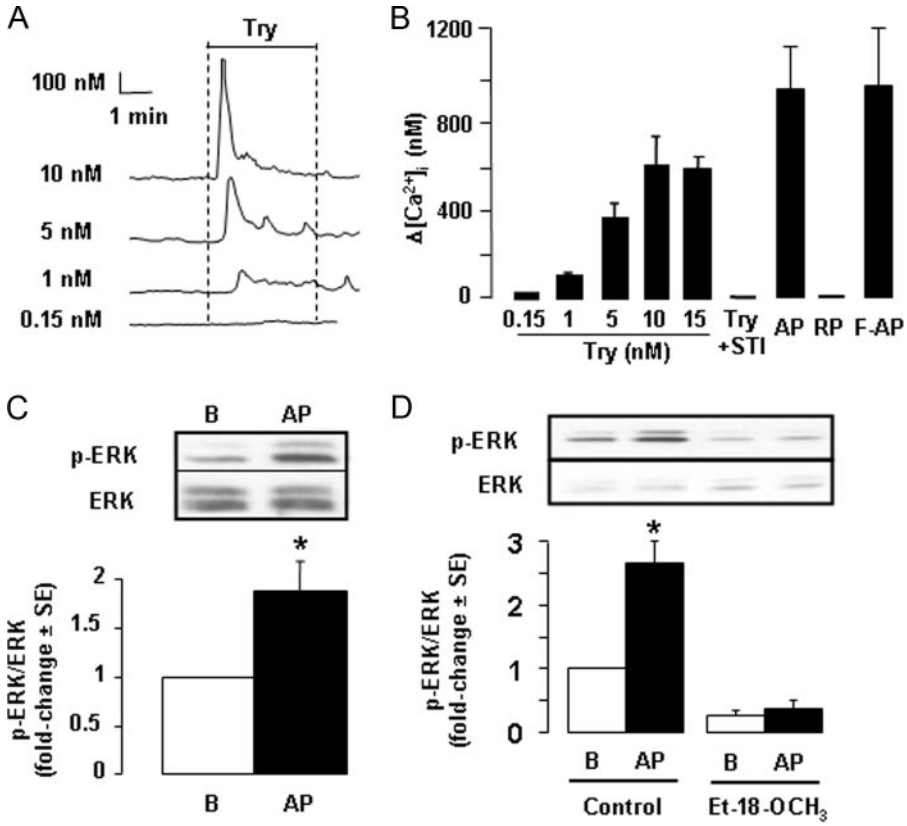

FIGURE 1. **PAR2 signaling in rat cTAL.** *A*, representative traces showing changes in $[Ca^{2+}]_i$ ($\Delta[Ca^{2+}]_i$) in cTAL, determined by fura 2-AM fluorescence, in response to basolateral addition of different concentrations of trypsin (Try). *B*, comparative effects on $[Ca^{2+}]_i$ of different concentrations of Try, 40 μM PAR2 AP, 40 μM inactive RP, 10 μM F-AP, or 20 nM soybean trypsin inhibitor and 10 nM trypsin (*Try + STI*). Data are means ± S.E. from 4–6 experiments. *C*, representative immunoblot and mean increase in the phosphoERK (*p-ERK*)/ERK ratio on cTAL incubated for 10 min at 37 °C under basal conditions (*B*) or in the presence of 40 μM PAR2 AP. Values are means ± S.E. from 8 experiments. *, $p < 0.001$ as compared with basal condition by Student's *t* test. *D*, same as in *C* in cTALs preincubated 45 min at 30 °C in the absence (control) or presence of 150 μM PLC inhibitor Et-18-OCH_3. Values are means ± S.E. from 4 experiments. *, $p < 0.001$ as compared with basal by Student's *t* test.

reabsorbs sodium via both the transcellular and the paracellular route. Transcellular NaCl reabsorption is primarily energized by basolateral Na,K-ATPase and generates a lumen-positive transepithelial potential difference (PD_{te}) that serves as driving force for paracellular sodium reabsorption (17). Thus, sodium reabsorption in cTAL was evaluated through monitoring of the PD_{te}, the conductance of the paracellular shunt pathway and the activity of Na,K-ATPase. Signaling events were evaluated pharmacologically.

EXPERIMENTAL PROCEDURES

Animals—Experiments were performed on male Sprague-Dawley rats (Charles River, L'Arbresle, France) weighing either 60–80 g for *in vitro* microperfusion experiments and intracellular calcium ($[Ca^{2+}]_i$) measurements or 160–180 g for Na,K-ATPase assay and immunoblotting. In preliminary experiments, we found no difference in Na,K-ATPase response to PAR2 activation between the two groups of rats (data not shown). Animals were fed the standard laboratory diet *ad libitum* with free access to tap water. All experiments were performed in accordance with the French legislation for animal care and experimentation.

Microdissection of cTAL—cTALs were dissected either from fresh kidney slices (microperfusion and $[Ca^{2+}]_i$ measurements) as described previously (18) or from liberase-treated kidneys (Na,K-ATPase measurement and immunoblotting). Kidney treatment with liberase (Blendzyme 2, Roche Diagnostics, Meylan, France) was designed so as to make microdissection of the large number of cTALs required for the different assays compatible with the preservation of PAR activity. Briefly, the left kidney was perfused *in situ* with 6 ml of Hank's solution supplemented with 1 mM glutamine, 1 mM pyruvate, 0.5 mM $MgCl_2$, 0.1% bovine serum albumin, 20 mM Hepes, and 0.015% liberase (w/v), pH 7.4. Thin pyramids were cut from the kidney and incubated in 0.006% liberase solution for 20–25 min at 30 °C and thoroughly rinsed in microdissection solution supplemented with inhibitors of protease (2 μg/ml aprotinin and 5 μg/ml leupeptin). Preliminary studies showed that this treatment reduced PAR2 peptidic agonist-induced increase in ($[Ca^{2+}]_i$) by 65%, but nevertheless, allowed us to detect 2-fold stimulations of Na,K-ATPase activity and of ERK phosphorylation in response to PAR2 activation.

Measurement of $[Ca^{2+}]_i$—Intracellular calcium concentration was determined on single cTALs by the fura 2-AM fluorescence, as described previously (19). Briefly, after isolation, each cTAL loaded with acetoxymethyl ester of fura 2-AM (10 μM, 1 h at room temperature) was transferred to a perfusion chamber and immobilized by sucking each end within the tip of a holding micropipette. The peritubular fluid maintained at 37 °C was continuously exchanged at a rate of ~10 ml/min. After a 5–10-min equilibration, fura 2-AM fluorescence of ~15 cells was measured with a standard photometric setup (MSP 21, Zeiss). Tubule autofluorescence was subtracted from the fluorescence intensities of fura 2-AM at 340 and 380 nm. Values were calculated as described previously (19).

Na,K-ATPase Assay—Na,K-ATPase activity was determined using pools of 4–6 permeabilized cTALs by the previously described microassay (20). For determining the V_{max} of the enzyme, total ATPase activity was determined in a solution containing 120 mM NaCl, 5 mM KCl, 10 mM $MgCl_2$, 1 mM EDTA, 100 mM Tris-HCl, 10 mM Na_2ATP, and 5 nCi/μl [γ-^{32}P]ATP (2–10 Ci/mmol) at pH 7.4. For basal ATPase activity measurements, NaCl and KCl were omitted, Tris-HCl was 150 mM, and 2 mM ouabain was added. For determination of the sodium apparent affinity of Na,K-ATPase, cTALs were thoroughly rinsed in a sodium-free medium (100 mM choline chlo-

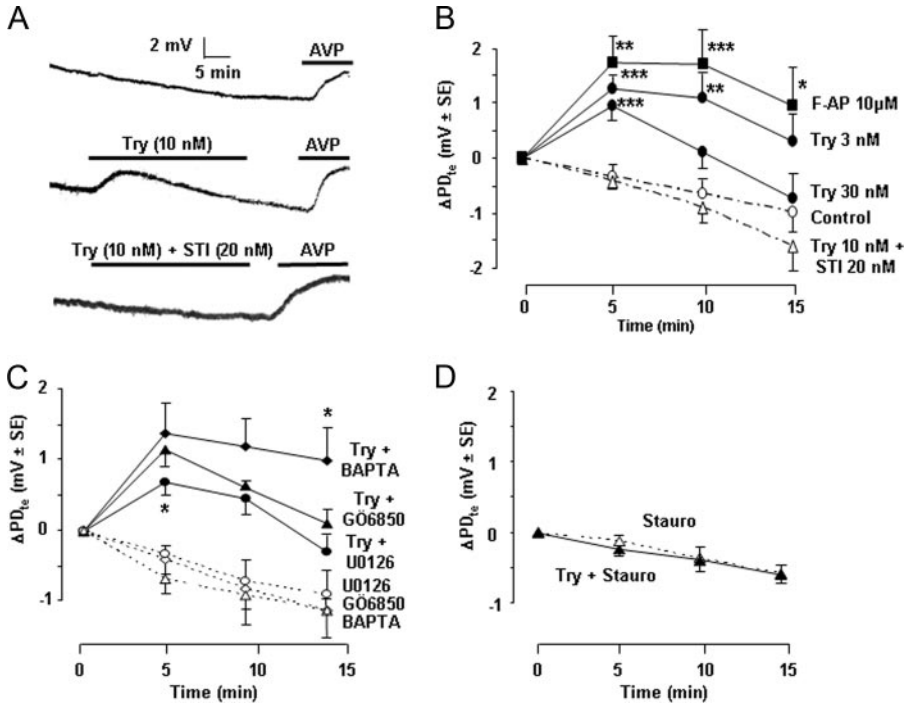

FIGURE 2. **Activation of PAR2 increases transepithelial voltage in rat cTAL.** *A*, representative traces showing the spontaneous variations of PD_{te} as a function of time (*top trace*) and the effect of Try (10 nM) addition to the bath in the absence (*middle trace*) or presence of soybean trypsin inhibitor (*STI*, 20 nM, *bottom trace*). The viability of each cTAL at the end of the experimental period was attested by the hyperpolarizing effect of the addition of 0.2 nM AVP to the bath. *B*, mean variation of PD_{te} (ΔPD_{te}) calculated 5, 10, and 15 min after the addition of Try or F-AP or in time control tubules. Values are means ± S.E. from 4–6 cTALs. Statistically significant differences between treated and time control cTALs: *, $p < 0.025$; **, $p < 0.01$; ***, $p < 0.005$. *C*, ΔPD_{te}, calculated as above, after the addition of trypsin (10 nM, *full lines*) or in time controls (*stippled lines*) in cTALs pretreated with BAPTA (10–20 μM, 1 h at room temperature before mounting in microperfusion chamber), GÖ6850 (100 nM, for at least 35 min during PD_{te} equilibration period), or U0126 (10 μM, for at least 35 min during the PD_{te} equilibration period). Values are means ± S.E. from 4–6 tubules. Statistically significant differences *versus* trypsin alone: *, $p < 0.025$. *D*, same as in *C* in cTALs pretreated with staurosporine (*Stauro*, 15 nM, for at least 35 min during PD_{te} equilibration period).

ride, 1 mM $CaCl_2$, 50 mM Tris-HCl, pH 7.4) after treatment with inhibitors and PAR2 agonists, and total ATPase activity was determined in a solution containing 10 mM $MgCl_2$, 1 mM EDTA, 100 mM Tris-HCl, 10 mM Tris-ATP, 5 nCi/μl [γ-^{32}P]ATP, and various concentrations of NaCl and KCl, the sum of their concentrations being maintained constant at 140 mM, at pH 7.4. Na,K-ATPase was taken as the difference between mean total and basal ATPase activities, each determined in triplicate. Values are means ± S.E. from several animals.

Cell Surface Expression of Na,K-ATPase—The abundance of cell surface Na,K-ATPase α subunit was quantified after cell surface biotinylation, streptavidin precipitation, and Western blotting, as described previously (21). Briefly, after treatment with or without agonist peptide SLIGRL-NH_2 (AP) (10 min at 37 °C), pools of 40 cTALs were incubated in bovine serum albumin-free microdissection solution containing 1.5 mg/ml EZ-Link Sulfo-NHS-SS-biotin (Pierce) for 60 min on ice, and thereafter, the biotin was quenched with 0.1% bovine serum albumin solution. Tubules were lysed in HB solution (20 mM Tris-HCl, pH 7.4, 2 mM EDTA, 2 mM EGTA, 1% Triton X-100, 0.1% SDS, protease inhibitor mixture (Roche Diagnostics)), and proteins were precipitated by 20% streptavidin agarose resin (Pierce) overnight at 4 °C in TLB solution (50 mM Tris-HCl, pH 7.4, 100 mM NaCl, 5 mM EDTA, protease inhibitor mixture (Roche Diagnostics)). The agarose resin was washed thrice in TLB solution and resuspended in Laemmli buffer. Proteins were denaturated for 15 min at 60 °C and separated on 7.5% acrylamide SDS-PAGE. Blots were successively incubated with anti-Na,K-ATPase α subunit antibody (1/10,000, gift from K. Geering) and anti-rabbit IgG horseradish peroxidase (1/10,000, Promega). In each experiment, duplicate samples were run in parallel. The densitometry of the ~100-kDa bands was quantitated by scanning and using the ImageJ software and normalized to cTAL length, and the mean value in AP-treated tubules was expressed as the percentage of that under basal conditions. Data are means from 4 experiments.

Immunoblotting—After treatment, pools of 50–80 cTALs were solubilized at 90 °C for 5 min after the addition of 1 volume of 2× Laemmli buffer. SDS-PAGE was performed on 10% polyacrylamide gels, and proteins were electrotransferred to polyvinylidene difluoride membranes (GE Healthcare). After blocking in TBS-Nonidet P-40 (50 mM Tris base, 150 mM NaCl, 0.2% Nonidet P-40) containing 10% low fat milk, blots were successively incubated with anti-ERK antibody (p44/42 MAP kinase antibody, Cell Signaling Technology, 1/500 in TBS-Nonidet P-40 + milk) and anti-rabbit IgG antibody coupled to horseradish peroxidase (Promega France, Charbonnières, France) and revealed with the Western Lightning chemiluminescence reagent Plus (PerkinElmer Life Sciences). After stripping (four successive incubations in 25 mM glycine pH 2, 0,2% SDS buffer), the polyvinylidene difluoride membranes were incubated with anti-phosphoERK antibody (phospho44/42 MAP kinase antibody, Cell Signaling Technology) and post-treated as above. Densitometry of the different bands was quantitated by scanning and using ImageJ software.

For each sample, the densitometry ratio of phosphoERK/ERK was calculated, and in each experiment, these ratios in different experimental conditions were expressed as the percentage of the control group. Data are means ± S.E. from several experiments.

In Vitro Microperfusion—cTALs dissected without liberase treatment were microperfused *in vitro* as described previously (18). Briefly, the dissected tubules were transferred to a perfusion chamber mounted on the stage of an inverted microscope and perfused by a gravity-driven system at a rate of ~15 nl/min. The bath flow rate was 12 ml/min to ensure a rapid and complete change of bath solutions, and its temperature was main-

TABLE 1

Effect of protein kinase inhibitors on trypsin-induced increase in PD_{te} in microperfused cTAL

cTALs were pretreated with inhibitors, at the indicated concentration, for at least 35 min during the PD_{te} equilibration period before stimulation with trypsin (10 nM). Changes in PD_{te} were recorded for at least 15 min after trypsin addition. Inhibitors targets and sensitivity (IC_{50} or K_i) are from the Calbiochem catalogue. Only targets possibly inhibited at inhibitor concentrations used in this study are listed. MEK, MAP kinase/ERK kinase; PTK, protein tyrosine kinases; PI3K, phosphatidylinositol 3-kinase.

Inhibitor	Concentration used	Target kinase	Sensitivity	Effect on try-induced increase in PD_{te}
	nM		nM	
Staurosporine	15	PKC	IC_{50} = 0.7	Full inhibition
		PKA	IC_{50} = 7	
		PKG	IC_{50} = 8.5	
		CaMK	IC_{50} = 20	
		MLC-K	IC_{50} = 1.3	
GÖ6850	100	PKCα, β, γ, δ, ϵ	K_i = 10	None
GÖ6983	1,000	PKCα, β, γ, δ	IC_{50} = 6–10	None
		PKCζ	IC_{50} = 60	
GÖ6976	200	PKCα, β	IC_{50} = 2 & 6	None
		PKCμ	IC_{50} = 20	
H89	500–1,000	PKA	K_i = 48	None
H8	2500	PKG	K_i = 480	None
ML7 hydrochloride	3,000	MLCK	K_i = 300	None
Autocamtide-2-related inhibitory peptide	40	CaMKII	IC_{50} = 4	None
U0126	10,000	$MEK_{1,2}$	IC_{50} = 72 & 58	Partial inhibition
Genistein	25,000–50,000	PTK	IC_{50} = 2–6000	None
Wortmanin	100	PI3K	IC_{50} = 5	None

tained at 37 °C. The PD_{te} was measured at the perfusion end of the tubule via microelectrodes connected through an Ag/AgCl half-cell to an electrometer.

In a first series of experiments, cTALs were perfused under symmetrical conditions. The bath and perfusate solutions contained (in mM): 118 NaCl, 23 $NaHCO_3$, 1.2 $MgSO_4$, 2 K_2HPO_4, 2 calcium lactate, 1 sodium citrate, 5.5 glucose, 5 alanine, 10 Hepes, pH 7.4 (bath continuously gassed with 95% O_2, 5% CO_2). In a second experimental series, cTAL were perfused in the presence of a NaCl diffusion gradient from the bath to the perfusate. For this purpose, the bath solution was unchanged, whereas NaCl concentration in the perfusate solution was reduced to 50 mM, and mannitol was added to achieve the same osmolarity.

Statistics—Results are expressed as means ± S.E. from several animals. Comparison between groups was performed either by non-paired *t* test or by variance analysis followed by protective least squares difference Fisher's test, as appropriate.

RESULTS

Expression of PAR2 in the cTAL—Because PAR2 are classically coupled to activation of PLC and calcium signaling, we attempted to demonstrate functional expression of PAR2 in the cTAL by searching for changes in $[Ca^{2+}]_i$ induced by activation of PAR2. Basolateral addition of trypsin to cTAL dose-dependently and transiently increased intracellular calcium concentration (Fig. 1, *A* and *B*), with threshold and maximal effects observed with 0.15 and 10 nM, respectively. This effect of trypsin was related to its proteolytic activity since it was abolished in the presence of soybean trypsin inhibitor (Fig. 1*B*). It was mimicked by the PAR2-specific AP and its furoylated derivative (F-AP) but not by the reverse inactive peptide LRGILS-NH_2 (RP) (Fig. 1*B*). Thrombin (1 μM), an agonist of PAR1, PAR3, and PAR4, was devoid of effect (data not shown). In the absence of extracellular calcium, the peak calcium response to trypsin was not altered (data not shown), demonstrating that it was accounted for by recruitment of an intracellular calcium pool.

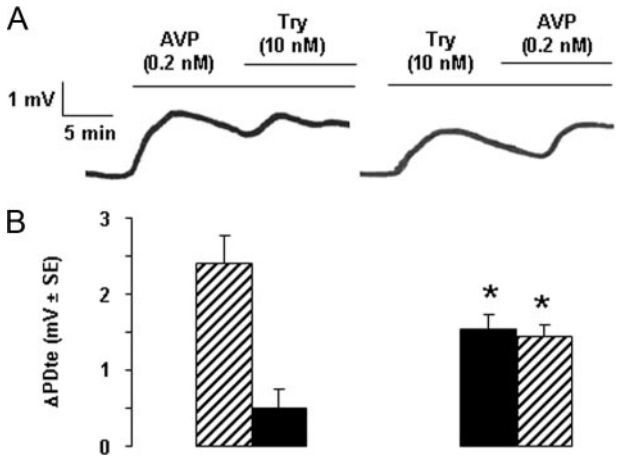

FIGURE 3. **Comparative effects of activation of PAR2 and vasopressin V2 receptor on transepithelial voltage in rat cTAL.** *A*, representative traces showing the effect on PD_{te} of the successive addition of vasopressin (AVP, 200 pM) followed by Try (10 nM) (*left trace*) or trypsin followed by AVP (*right trace*). *B*, mean variation of PD_{te}, calculated between the PD_{te} values at the peak response and at the time of trypsin (*dark columns*) or AVP (*hatched columns*) addition. *Left panel*, the addition of AVP followed by trypsin; *right panel*, the addition of trypsin followed by AVP. Values are means ± S.E. from 5–6 cTALs. *, $p < 0.01$ between the two experimental series.

Following a first stimulation by trypsin, PAR2 was rapidly desensitized (data not shown).

The addition of AP to cTAL increased almost 2-fold the phosphorylation level of $ERK_{1,2}$ (Fig. 1*C*). Pretreatment with the specific PLC inhibitor Et-18-OCH_3 (150 μM) decreased the basal phosphorylation of ERK and prevented its stimulation by AP (Fig. 1*D*). All together, these results demonstrate that rat cTAL expresses functional basolateral PAR2 coupled to PLC stimulation and subsequent activation of $ERK_{1,2}$.

Effect of PAR2 on Transepithelial Voltage—As described previously, *in vitro* microperfused rat cTAL displayed a lumen-positive PD_{te} that spontaneously decreased with time (Fig. 2, *A* and *B*), likely due to progressive turn off of *in vivo* stimulatory pathways. When a steady rate of PD_{te} decrease was achieved, at

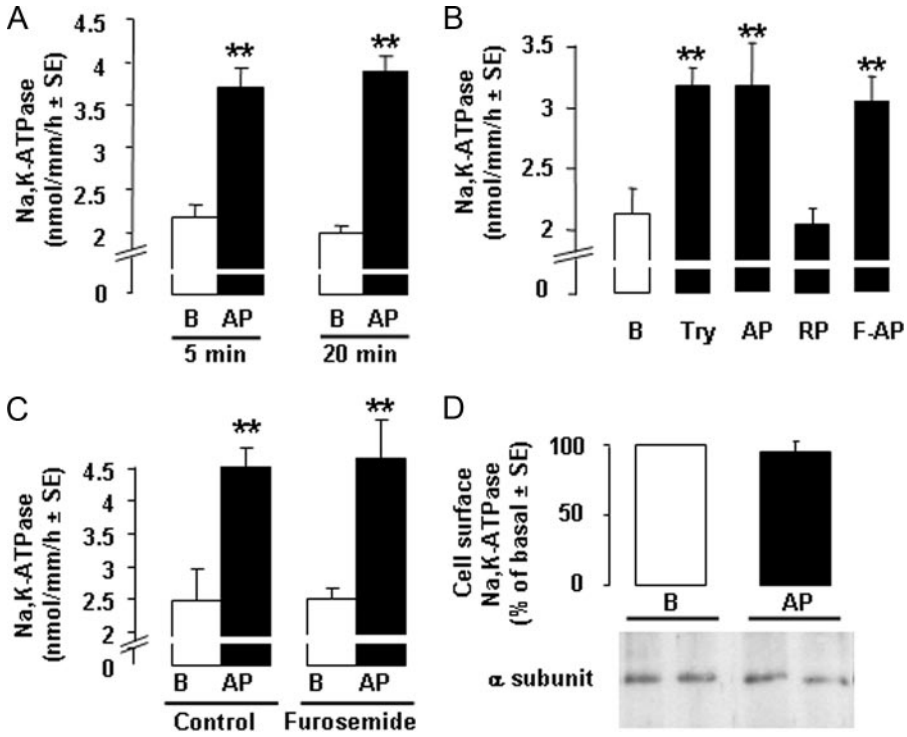

FIGURE 4. **Activation of PAR2 stimulates Na,K-ATPase V_{max} in the rat cTAL.** *A*, Na,K-ATPase V_{max} in cTAL incubated under basal conditions (*B*, *open columns*) or with 40 μM PAR2 AP (*dark columns*) for 5 or 20 min. Values are means ± S.E. from 4 (20 min) and 13 (5 min) animals. **, $p < 0.001$ as compared with basal. *B*, representative experiment showing Na,K-ATPase V_{max} in cTAL incubated for 5 min at 37 °C in basal condition *B* or in the presence of 10 nM Try, 40 μM PAR2 AP, 40 μM inactive RP, or 10 μM F-AP. **, $p < 0.001$ as compared with basal. *C*, Na,K-ATPase activity in cTALs incubated for 5 min at 37 °C with or without 40 μM AP (*B* and *AP*, respectively) in the absence (*Control*) or presence of 100 μM furosemide. Values are means ± S.E. from 3 experiments. **, $p < 0.001$ as compared with basal. *D*, representative immunoblot and mean change in plasma membrane expression of Na,K-ATPase α subunit in cTAL incubated for 10 min at 37 °C under basal conditions (*B*) or in the presence of 40 μM PAR2 AP. Membrane Na,K-ATPase was quantified by Western blotting after biotin labeling and streptavidin precipitation. Values are means ± S.E. from 4 experiments.

~0.07 mV/min (residual PD_{te} = 8.3 ± 0.6 mV ± S.E., n = 30), the addition of trypsin (3–10 nM) to the perfusion bath increased PD_{te} by ~1.5 mV within 5 min (Fig. 2, *A* and *B*). Thereafter, PD_{te} decreased at the same rate as spontaneously observed in time control cTALs. Consequently, trypsin-induced hyperpolarization remained almost constant for at least 15 min. In contrast, at a higher trypsin concentration (30 nM), the decrease was more rapid, and the PD_{te} returned to time control level within 15 min (Fig. 2*B*). Like low trypsin concentrations, F-AP induced a stable hyperpolarization. The hyperpolarizing effect of trypsin was abolished by soybean trypsin inhibitor (Fig. 2, *A* and *B*).

The hyperpolarizing effect of trypsin was not altered by BAPTA, which buffers changes in intracellular calcium concentration. It was also insensitive to specific inhibitors of all classical (cPKCs), novel, and atypical PKCs known to be expressed in TAL (22–24) and was only mildly inhibited by the $ERK_{1,2}$ kinase inhibitor U0126 (Fig. 2*C* and Table 1). Inhibitors of cAMP- and cGMP-dependent protein kinases (PKA and PKG), calmodulin kinase (CaMK), myosin light chain kinase (MLC-K), protein tyrosine kinases, and phosphatidylinositol-3 kinase (*i.e.* other signaling pathways triggered by PAR2 in different cell types (4)) were also devoid of effect (Table 1). However, total prevention of trypsin-induced hyperpolarization of cTAL could be achieved with a low concentration of staurosporine (15 nM), a broad spectrum inhibitor of serine threonine kinases (Fig. 2*D*). Thus, trypsin-induced hyperpolarization of cTAL is not mediated by the classical PLC/Ca^{2+}/cPKC/ERK-dependent signaling pathway but by a calcium-independent pathway involving an unidentified staurosporine-sensitive kinase.

The addition of vasopressin (AVP), at a concentration that induces a maximal increase in PD_{te} via activation of its V2 receptors and activation of PKA in rat TAL, increased the PD_{te} by ~2.5 mV. Subsequent addition of trypsin, during AVP-induced stimulation, further increased PD_{te}, but only by 0.5 mV, *i.e.* to a lesser extent than trypsin alone (Fig. 3, *A* and *B*). Conversely, the addition of vasopressin during the plateau response to trypsin increased PD_{te} by only 1.5 mV, which is less than the initial response to AVP (Fig. 3, *A* and *B*). This demonstrates a partial additivity of PD_{te} responses to stimulation of AVP V2 receptor and PAR2. Because these two receptors are coupled to a different signaling pathway, the partial additivity of their effects on PD_{te} suggests that these effects result in part from the stimulation of at least one common target.

Effect of PAR2 Stimulation on Na,K-ATPase—Treatment of cTALs with AP increased the V_{max} of Na,K-ATPase by >80% within 5 min, and this stimulation was sustained for at least 20 min (Fig. 4*A*). Stimulation of Na,K-ATPase V_{max} was also observed in response to trypsin and F-AP, whereas RP had no effect (Fig. 4*B*), indicating that it was secondary to activation of PAR2. Furosemide, a specific and potent inhibitor of apical sodium entry in cTAL, did not alter the stimulatory effect of AP on Na,K-ATPase V_{max} (Fig. 4*C*), demonstrating that stimulation of Na,K-ATPase is a primary effect of PAR2 activation and is not secondary to increased sodium entry, an event known to trigger targeting of cytosolic Na,K-ATPase subunits at the plasma membrane (25). AP-induced increase in Na,K-ATPase V_{max} was not associated with any increase in the expression of Na,K-ATPase α subunit at the plasma membrane (Fig. 4*D*). In addition to its stimulatory action on Na,K-ATPase V_{max}, AP also enhanced about 2-fold the apparent affinity of Na,K-ATPase for sodium, from ~40 to ~20 mM (Fig. 5*A* and Table 2).

Inhibition of PLC with Et-18-OCH_3 (150 μM) prevented the increase in Na,K-ATPase V_{max} and apparent affinity for sodium (Fig. 5*B* and Table 2). This inhibitory action of Et-18-OCH_3 was not related to a toxic, nonspecific effect since it did not alter cAMP-induced stimulation of Na,K-ATPase (data not shown). AP-induced stimulation of Na,K-ATPase V_{max} was also abolished by blunting changes in intracellular calcium with BAPTA

(10 μM), by inhibiting classical PKCs (PKCα, PKCβ) by GÖ6976 (200 nM) and $ERK_{1,2}$ kinase by U0126 (10 μM) (Fig. 5, *C–E*, and Table 2). In contrast, AP-induced increase in sodium affinity was not prevented either by BAPTA or by GÖ6976 or U0126 (Fig. 5, *C–E*, and Table 2). It was abolished by the wide spectrum kinase inhibitor staurosporine (Fig. 5*F* and Table 2).

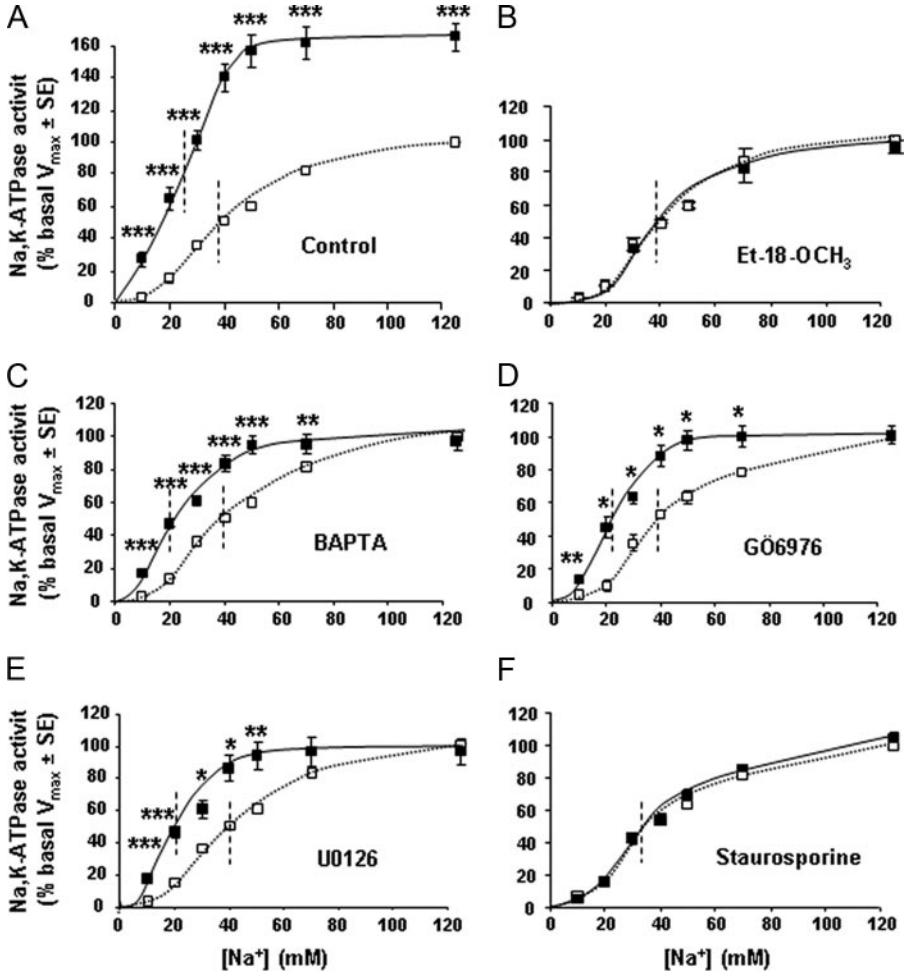

FIGURE 5. **Activation of PAR2 increases Na,K-ATPase apparent affinity for sodium in the rat cTAL.** *A–F*, sodium dependence of Na,K-ATPase activity in cTALs preincubated for 45 min at 30 °C with either diluent (*A*, control) or 150 μM Et-18-OCH_3 (*B*), 10 μM BAPTA (*C*), 200 nM GÖ6976 (*D*), 10 μM U0126 (*E*), or 15 nM staurosporine (*F*) before being incubated for 10 min at 37 °C with (*solid line*) or without 40 μM AP (*dotted line*). In each experiment, Na,K-ATPase activities at different Na^+ concentrations were calculated as the percentage of the activity determined in the presence of 125 mM Na^+ (V_{max}) under basal condition (absence of AP). Values are means ± S.E. from 3–5 experiments. *, $p < 0.025$; **, $p < 0.005$, ***, $p < 0.001$ as compared with basal conditions.

All together, these findings demonstrate that PAR2-induced activation of PLC has dual effects on Na,K-ATPase in rat cTAL. Firstly, it increases its V_{max} activity via a signaling cascade that includes increased intracellular calcium concentration, stimulation of PKCα/β, and phosphorylation of $ERK_{1,2}$. Positive regulation of Na,K-ATPase by $ERK_{1,2}$ has already been reported in the renal collecting duct (26). Stimulation of Na,K-ATPase V_{max} activity by PKCα has also been observed in TAL in response to insulin-connecting peptide (24). Secondly, PAR2 activation unexpectedly increases Na,K-ATPase apparent affinity for sodium via a different, although PLC-dependent, pathway, which is independent of increased intracellular calcium, of PKCα/β, and of $ERK_{1,2}$ but sensitive to staurosporine, as is the trypsin-induced increase in PD_{te}. Based on these data, we conclude that the increase in sodium apparent affinity of Na,K-ATPase is a key component of the PAR2-induced increase in cTAL transepithelial PD_{te} that involves a calcium-independent staurosporine-sensitive kinase, the nature of which remains to be determined.

Effect of PAR2 on Paracellular Ion Permeability—To measure the paracellular permeability to sodium, the transcellular transport of NaCl was blocked by the addition of luminal furosemide (100 μM), and a diffusion gradient for NaCl was established between the bath and the lumen through partial substitution of perfusate NaCl with mannitol (Fig. 6*A*). Under these conditions, cTALs displayed a steady lumen-positive PD_{te} (18.7 ± 0.9 mV ± S.E., $n = 13$), generated by the diffusion of bath sodium to the cTAL lumen through the paracellular pathway. This lumen-positive potential con-

TABLE 2

Effect of PAR2 stimulation on Na,K-ATPase kinetic properties in rat cTAL

After preincubation for 45 min at 30 °C with either diluent (control) or 150 μM Et-18-OCH_3, 10 μM BAPTA, 200 nM GO6976, 15 nM staurosporine, or 10 μM U0126, cTALs were incubated at 37 °C for 10 min with or without 40 μM PAR2 AP. Thereafter, Na,K-ATPase activity was determined in the presence of increasing concentrations of sodium (as in Fig. 5). In each experiment, values were fitted to the Hill equation, considering that the activity determined with 125 mM sodium was the V_{max}, and the n_{Hill} and apparent affinity for sodium ($K_{0.5}$) were calculated. Values are means ± S.E. from 3–5 experiments. Statistically significant differences between AP-treated and -untreated (basal) cTALs: *, $p < 0.001$.

	Basal			AP		
	V_{max}	n_{Hill}	$K_{0.5}$	V_{max}	n_{Hill}	$K_{0.5}$
Control	1.9 ± 0.1	2.6 ± 0.2	39.8 ± 0.7	3.0 ± 0.2*	2.9 ± 0.3	20.8 ± 0.8*
Et-18-OCH_3	1.8 ± 0.3	2.7 ± 0.1	42.0 ± 0.9	1.7 ± 0.3	2.5 ± 0.1	40.4 ± 0.4
BAPTA	2.2 ± 0.2	2.5 ± 0.1	39.5 ± 0.5	2.1 ± 0.1	3.3 ± 0.3	19.0 ± 0.5*
GÖ6976	2.2 ± 0.5	2.4 ± 0.2	40.7 ± 0.6	2.2 ± 0.2	3.1 ± 0.2	20.5 ± 0.7*
Staurosporine	2.5 ± 0.2	2.2 ± 0.1	36.6 ± 0.2	2.6 ± 0.3	2.4 ± 0.1	37.8 ± 0.9
U0126	2.1 ± 0.1	3.1 ± 0.6	39.7 ± 1.0	2.0 ± 0.2	3.0 ± 0.1	19.0 ± 0.5*

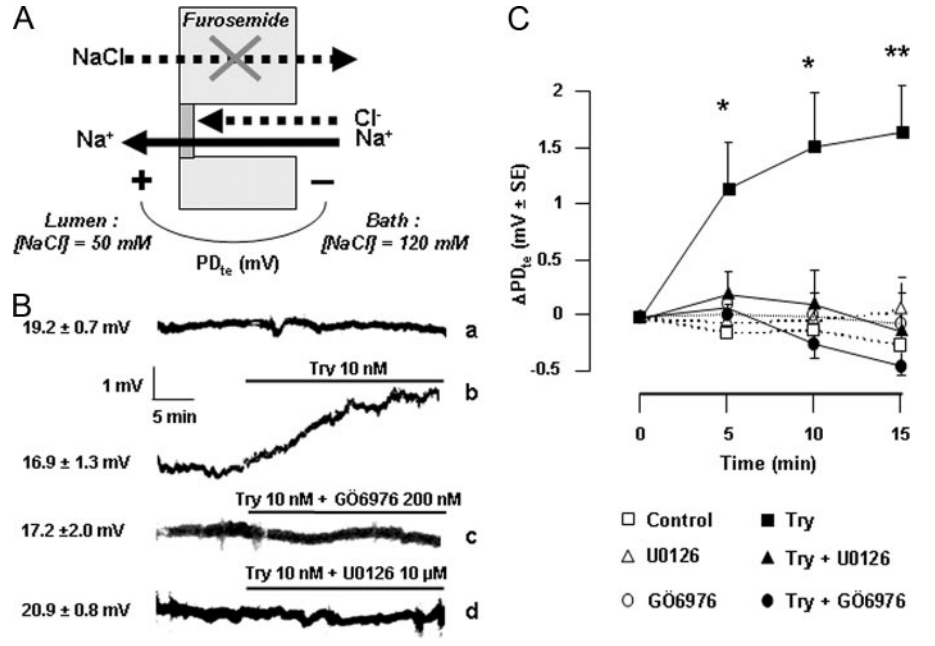

FIGURE 6. **Activation of PAR2 increases the paracellular sodium permeability.** *A*, cTALs were microperfused *in vitro* in the presence of 100 μM furosemide (to fully inhibit transcellular NaCl transport) and of a NaCl concentration gradient between the bath and the luminal fluid (NaCl bath, 120 mM; NaCl perfusate, 50 mM). Under these conditions, the PD_{te} is generated by the conductive diffusion of Na^+ and/or Cl^- ions from the bath to the lumen through the paracellular pathway. *B*, the positivity of the mean PD_{te} is accounted for by the much higher permeability of the paracellular pathway to sodium than to chloride. *Trace a* shows that conversely to the PD_{te} generated by transcellular transport (Fig. 2), this sodium diffusion-generated PD_{te} is stable as a function of time. The addition of Try (10 nM) to the bath increases the PDte (*trace b*), and the effect of trypsin is abolished in the presence of 200 nM GÖ6976 (*trace c*) or 10 μM U0126 (*trace d*). *C*, mean ΔPD_{te} values in cTAL preincubated or not with 200 nM GÖ6976 or 10 μM U0126 and treated (*solid lines*) or not (*dotted lines*) with 10 nM Try. Values are means ± S.E. from 4–7 cTALs. *, $p < 0.01$; **, $p < 0.005$ as compared with controls.

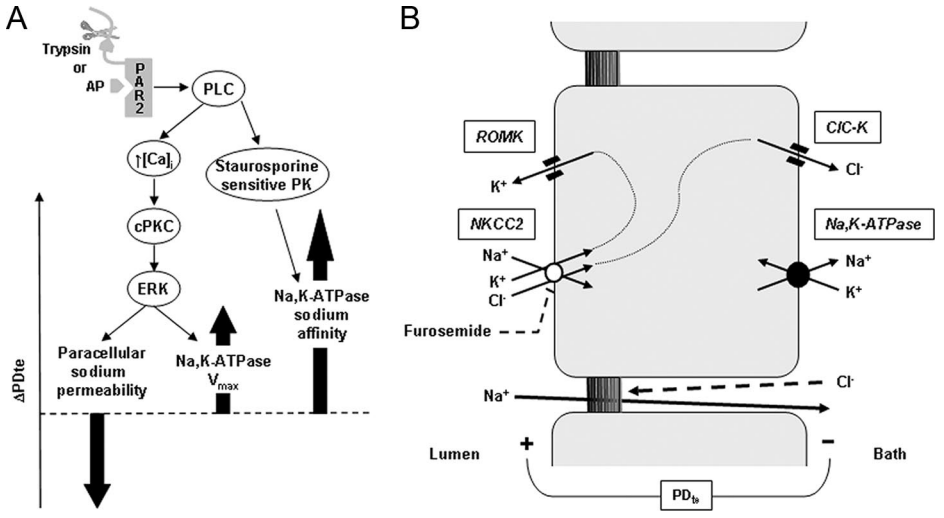

FIGURE 7. **Regulation of sodium transport by PAR2 in the rat cTAL.** *A*, activation of basolateral PAR2, either by cleavage of its N-terminal domain by trypsin or by a synthetic peptide mimicking the ligand domain, is coupled to the activation of PLC. In turn, PLC triggers calcium signaling ($\uparrow [Ca^{2+}]_i$), which activates cPKc and induces the phosphorylation of ERK. Activation of ERK is responsible both for increased permeability of the tight junction to sodium and for enhanced V_{max} of Na,K-ATPase. Because inhibition of this pathway has no significant effect on the transepithelial voltage (PD_{te}), it is suggested that the opposite effects on PD_{te} of increased V_{max} of Na,K-ATPase and increased permeability to sodium of the paracellular pathway (*thick arrows*) are quantitatively similar. Activation of PLC also stimulates an unidentified staurosporine-sensitive protein kinase, which mediates an increase in the apparent affinity of Na,K-ATPase for sodium. Because inhibition of this pathway also abolishes PAR2-induced increase in PD_{te}, the increased sodium affinity of Na,K-ATPase is likely a major actor of the change in PD_{te} and to increased sodium reabsorption. *B*, basolateral Na,K-ATPase generates a sodium gradient allowing apical entry of sodium, potassium, and chloride via the furosemide-sensitive cotransporter NKCC2. Diffusive exit of potassium by apical ROMK and of chloride by basolateral ClC-K generates a transepithelial voltage (PD_{te}) that drives paracellular reabsorption of sodium. Because the tight junctions are almost impermeable to chloride, there is no back diffusion of chloride toward the lumen.

firmed the preferential conductance of the paracellular pathway for sodium over chloride (17). After the addition of trypsin to the bath, the PD_{te} increased by >1.5 mV within 10 min (Fig. 6, *B* and *C*), indicating increased permeability of the paracellular pathway preferentially for sodium.

This effect of trypsin on the paracellular conductance to sodium was fully blocked in the presence of inhibitors of the classical PKCs (GÖ6976) and of ERK kinase (U0126) (Fig. 6, *B* and *C*). Because inhibition of PLC fully abolished PAR2-induced phosphorylation of $ERK_{1,2}$, the effect of PAR2 on paracellular sodium permeability is likely mediated by the same PLC/PKC/ERK cascade as that mediating the increase in Na,K-ATPase V_{max}. In the light of these data, the lack of effect of cPKC inhibition on PAR2-induced increase in PD_{te} (Fig. 2*C*) suggests that the increase in PD_{te} brought about by the stimulation of Na,K-ATPase V_{max} is counterbalanced by its decrease related to stimulation of paracellular permeability (Fig. 7*A*).

DISCUSSION

Sodium reabsorption in TAL occurs via both the transcellular and the paracellular routes (Fig. 7*B*). The sodium gradient generated by basolateral Na,K-ATPase in TAL cells is mainly dissipated by the apical, furosemide-sensitive, electroneutral Na/K/2Cl cotransport system (NKCC2) that couples the downhill entry of sodium to the uphill transport of potassium and chloride. Potassium ions accumulated above Nernst equilibrium within the cell by NKCC2 are recycled across the apical membrane via inwardly rectifying, voltage-insensitive potassium channels (ROMK). Chloride ions leave the cells across the basolateral membrane mainly via chloride channels (ClC-K). Conductive diffusion of chloride and potassium depolarizes the basolateral membrane and hyperpolarizes the apical one, respectively. These two diffusion potentials in series

combine to generate a lumen-positive transepithelial voltage characterizing the TAL. This transepithelial voltage is the driving force for paracellular ion transport; because the permeability of the paracellular route is higher for cations than for anions, the shunt current is mainly carried by net sodium reabsorption.

Present results go to prove that activation of PAR2 stimulates both transcellular and paracellular sodium reabsorption in the rat cTAL. Trypsin and PAR2-specific peptide agonist not only increase the transepithelial voltage (Fig. 2), reflecting increased transcellular reabsorption of NaCl, but also the paracellular permeability to sodium (Fig. 6). In the presence of a physiological lumen-positive transepithelial voltage, this enhanced sodium conductance increases the amount of sodium reabsorbed through the shunt pathway. This effect is further amplified by the concomitant increase in transepithelial voltage brought about by the stimulation of transcellular transport.

Although PAR2-induced changes in paracellular permeability are mediated by the PLC/cPKC/ERK pathway in cTAL (Fig. 6), as in intestine and corneal epithelia (27, 28), they display different features. 1) Paracellular permeability increases within minutes following activation of PAR2 in cTAL (Fig. 6) but only after hours in other epithelia (27–29). 2) PAR2 stimulation induces intracellular redistribution of the tight junction protein ZO-1 in intestine, whereas we did not observe such an event in a TAL cell line that expresses PAR2 (data not shown). 3) Along with this last finding, changes in cTAL are more subtle as they mostly concern the selectivity of the paracellular pathway to sodium, whereas they result in major alterations of the barrier function of tight junctions in other epithelia, allowing, for example, the transepithelial crossing of macromolecules and possibly of bacteria (27, 29). These findings suggest that the molecular targets of PAR2 pathway in TAL tight junctions are the proteins specifically responsible for their ion permselectivity, such as claudins, rather than the ubiquitous structural proteins.

Increased transcellular reabsorption of NaCl in TAL can be accounted for by stimulation of Na,K-ATPase, ClC-K, ROMK, or NKCC2. In the present study, we documented marked increases in both the V_{max} (Fig. 4) and the apparent affinity for sodium of Na,K-ATPase (Fig. 5 and Table 2), two events subsequent to PLC activation (Fig. 7). PAR2-induced stimulation of Na,K-ATPase V_{max} is independent of increased apical sodium entry (Fig. 4*C*), suggesting a primary regulation of the pump by trypsin-like proteases. This does not exclude that besides Na,K-ATPase, ROMK, ClC-K, and/or NKCC2 may also be target(s) of PAR2. As a matter of fact, PAR2 activation of chloride and potassium channels has already been reported in secretory epithelia (12–16).

It has been shown previously that membrane translocation of PKCα by insulin-connecting peptide increases the V_{max} of Na,K-ATPase in medullary TAL, without altering the number of units located at the plasma membrane (24). This suggests that C peptide increases the maximal turnover rate of pre-existing Na,K-ATPase units. Since PAR2 activation does not increase the abundance of Na,K-ATPase at the cell surface (Fig. 4*D*), a similar mechanism might account for the increased Na,K-ATPase V_{max} induced here by PAR2 via PLC, cPKC, and ERK (Fig. 5). However, in another study on rat medullary TAL, activation of PKCα by superoxides has been shown to stimulate NKCC2 without associated change in Na,K-ATPase activity (23, 30). This indicates that other cellular events should occur together with activation of PKCα to account for the agonist specificity of the TAL response.

Increased affinity of Na,K-ATPase for sodium has been described before in the proximal tubule (31, 32) but not in the TAL. Interestingly, PAR2-induced increase in Na,K-ATPase affinity for sodium is secondary to activation of PLC, but it is independent of changes in $[Ca^{2+}]_i$ and insensitive to inhibitors of classical PKCs, depending on a yet unidentified staurosporine-sensitive kinase, (Fig. 5 and Table 1), as transepithelial voltage (Fig. 2).

Functionally, the dual stimulation of Na,K-ATPase allows increased transcellular reabsorption of sodium even in the presence of reduced intracellular sodium concentration, *i.e.* in the absence of primary stimulation of apical sodium entry via NKCC2. This mechanism is different from that induced by the AVP-induced cAMP/PKA pathway, which primarily relies on activation of apical sodium entry, secondarily to phosphorylation and targeting of NKCC2 to the apical plasma membrane (33). Therefore, cAMP-generating agonists and PAR2-activating proteases, by stimulating distinct signaling pathways in the same cell, may be expected to cooperate in enhancing NaCl transport in TAL. In support of this hypothesis, trypsin and AVP were found to induce partially additive effects on PD_{te} in *in vitro* microperfused cTAL (Fig. 3). *In vivo*, sodium transport in TAL is under strong stimulatory regulation by multiple hormones and receptors that maintain the cyclic AMP/PKA pathway under maximal activation (34, 35). Therefore, PAR2-activating proteases may currently be considered as the sole agonist capable of increasing TAL transport capacity, under *in vivo* conditions. The proteases that may activate kidney PAR2 have not been searched for in this study. Trypsin is unlikely a physiologically relevant stimulus, but several circulating serine proteases displaying trypsin-like activity are putative candidates. Alternately, renal kallikrein is a good candidate since it is secreted by neighboring connecting tubules (36) and is able to activate PAR2 (37).

Acknowledgment—We are grateful to Dr. Soline Bourgeois (Institut des Cordeliers, Paris) for immunohistochemical study of protein ZO-1 in TAL cells.

REFERENCES

1. Ossovskaya, V. S., and Bunnett, N. W. (2004) *Physiol. Rev.* **84,** 579–621
2. Fyfe, M., Bergstrom, M., Aspengren, S., and Peterson, A. (2005) *Cytokine* **31,** 358–367
3. Kawao, N., Nagataki, M., Nagasawa, K., Kubo, S., Cushing, K., Wada, T., Sekiguchi, F., Ichida, S., Hollenberg, M. D., MacNaughton, W. K., Nishikawa, H., and Kawabata, A. (2005) *J. Pharmacol. Exp. Ther.* **315,** 576–589
4. Nishibori, M., Mori, S., and Takahashi, H. K. (2005) *J. Pharmacol. Sci.* **97,** 25–30
5. Bertog, M., Letz, B., Kong, W., Steinhoff, M., Higgins, M. A., Bielfeld-Ackermann, A., Fromter, E., Bunnett, N. W., and Korbmacher, C. (1999) *J. Physiol.* (*Lond.*) **521,** 3–17
6. Bohm, S. K., Kong, W., Bromme, D., Smeekens, S. P., Anderson, D. C., Connolly, A., Kahn, M., Nelken, N. A., Coughlin, S. R., Payan, D. G., and

Bunnett, N. W. (1996) *Biochem. J.* **314,** 1009–1016
7. Grandaliano, G., Pontrelli, P., Cerullo, G., Monno, R., Ranieri, E., Ursi, M., Loverre, A., Gesualdo, L., and Schena, F. P. (2003) *J. Am. Soc. Nephrol.* **14,** 2072–2083
8. Xu, Y., Zacharias, U., Peraldi, M. N., He, C. J., Lu, C., Sraer, J. D., Brass, L. F., and Rondeau, E. (1995) *Am. J. Pathol.* **146,** 101–110
9. Cunningham, M. A., Rondeau, E., Chen, X., Coughlin, S. R., Holdsworth, S. R., and Tipping, P. G. (2000) *J. Exp. Med.* **191,** 455–462
10. Rondeau, E., Vigneau, C., and Berrou, J. (2001) *Nephrol. Dial. Transplant.* **16,** 1529–1531
11. Gui, Y., Loutzenhiser, R., and Hollenberg, M. D. (2003) *Am. J. Physiol.* **285,** F95–F104
12. Cuffe, J. E., Bertog, M., Velazquez-Rocha, S., Dery, O., Bunnett, N., and Korbmacher, C. (2002) *J. Physiol.* (*Lond.*) **539,** 209–222
13. Danahay, H., Withey, L., Poll, C. T., van de Graaf, S. F., and Bridges, R. J. (2001) *Am. J. Physiol.* **280,** C1455–C1464
14. Kunzelmann, K., Schreiber, R., Konig, J., and Mall, M. (2002) *Cell Biochem. Biophys.* **36,** 209–214
15. Kunzelmann, K., Sun, J., Markovich, D., Konig, J., Murle, B., Mall, M., and Schreiber, R. (2005) *FASEB J.* **19,** 969–970
16. Nguyen, T. D., Moody, M. W., Steinhoff, M., Okolo, C., Koh, D. S., and Bunnett, N. W. (1999) *J. Clin. Investig.* **103,** 261–269
17. Greger, R. (1985) *Physiol. Rev.* **65,** 760–797
18. de Jesus Ferreira, M. C., and Bailly, C. (1997) *J. Physiol.* (*Lond.*) **505,** 749–758
19. Champigneulle, A., Siga, E., Vassent, G., and Imbert-Teboul, M. (1993) *Am. J. Physiol.* **265,** F35–F45
20. Deschenes, G., and Doucet, A. (2000) *J. Am. Soc. Nephrol.* **11,** 604–615
21. Vinciguerra, M., Deschenes, G., Hasler, U., Mordasini, D., Rousselot, M., Doucet, A., Vandewalle, A., Martin, P. Y., and Feraille, E. (2003) *Mol. Biol. Cell* **14,** 2677–2688
22. Aristimuno, P. C., and Good, D. W. (1997) *Am. J. Physiol.* **272,** F624–F631
23. Silva, G. B., Ortiz, P. A., Hong, N. J., and Garvin, J. L. (2006) *Hypertension* **48,** 467–472
24. Tsimaratos, M., Roger, F., Chabardes, D., Mordasini, D., Hasler, U., Doucet, A., Martin, P. Y., and Feraille, E. (2003) *Diabetologia* **46,** 124–131
25. Barlet-Bas, C., Khadouri, C., Marsy, S., and Doucet, A. (1990) *J. Biol. Chem.* **265,** 7799–7803
26. Michlig, S., Mercier, A., Doucet, A., Schild, L., Horisberger, J. D., Rossier, B. C., and Firsov, D. (2004) *J. Biol. Chem.* **279,** 51002–51012
27. Jacob, C., Yang, P. C., Darmoul, D., Amadesi, S., Saito, T., Cottrell, G. S., Coelho, A. M., Singh, P., Grady, E. F., Perdue, M., and Bunnett, N. W. (2005) *J. Biol. Chem.* **280,** 31936–31948
28. Wang, Y., Zhang, J., Yi, X. J., and Yu, F. S. (2004) *Exp. Eye Res.* **78,** 125–136
29. Cenac, N., Chin, A. C., Garcia-Villar, R., Salvador-Cartier, C., Ferrier, L., Vergnolle, N., Buret, A. G., Fioramonti, J., and Bueno, L. (2004) *J. Physiol.* (*Lond.*) **558,** 913–925
30. Juncos, R., and Garvin, J. L. (2005) *Am. J. Physiol.* **288,** F982–F987
31. Feraille, E., Carranza, M. L., Buffin-Meyer, B., Rousselot, M., Doucet, A., and Favre, H. (1995) *Am. J. Physiol.* **268,** C1277–C1283
32. Ohtomo, Y., Aperia, A., Sahlgren, B., Johansson, B. L., and Wahren, J. (1996) *Diabetologia* **39,** 199–205
33. Ortiz, P. A. (2006) *Am. J. Physiol.* **290,** F608–F616
34. Feraille, E., and Doucet, A. (2001) *Physiol. Rev.* **81,** 345–418
35. Morel, F., and Doucet, A. (1986) *Physiol. Rev.* **66,** 377–468
36. Marchetti, J., Imbert-Teboul, M., Alhenc-Gelas, F., Allegrini, J., Menard, J., and Morel, F. (1984) *Pfluegers Arch. Eur. J. Physiol.* **401,** 27–33
37. Oikonomopoulou, K., Hansen, K. K., Saifeddine, M., Vergnolle, N., Tea, I., Blaber, M., Blaber, S. I., Scarisbrick, I., Diamandis, E. P., and Hollenberg, M. D. (2006) *Biol. Chem.* **387,** 817–824